

Controlling Dimensions of Polymerized Micelles: Micelle Template versus Reaction Conditions

Michael J. Gerber and Lynn M. Walker*

Department of Chemical Engineering (Center for Complex Fluids Engineering),
Carnegie Mellon University, Pittsburgh, Pennsylvania 15213

Received August 23, 2005. In Final Form: November 7, 2005

The polymerization of elongated micellar structures offers a novel approach to the production of high aspect ratio, water-soluble amphiphilic nanoparticles. Three different surfactants were synthesized consisting of a cationic surfactant of the form (C_xH_{2x+1}) trimethylammonium (where $X = 14, 16$, or 18) and a vinyl-containing counterion, 4-vinylbenzoate. The resulting polymer–surfactant aggregates have been polymerized to produce high aspect ratio nanoparticles which are insensitive to changes in solution conditions. The radius of the initial template is maintained on polymerization, whereas the template length is not. The aggregate radius is varied by changing the length of the surfactant tail, in this case producing aggregates with radii of 1.7, 2.0, or 2.4 nm. Variation of the initiator decomposition half-life, by means of using different initiators and varying temperature, is used to control the aggregate length between 80 and 500 nm. Through the process discussed here, both the radius and length of the aggregates are controlled independently.

Introduction

The addition of hydrotropic counterions to ionic surfactant systems often leads to the formation of elongated, or wormlike, micelles at only a few times the critical micelle concentration.^{1–4} These wormlike micelles form viscoelastic solutions,^{5–7} retain the solubilizing properties common to surfactant systems, and, pertinent to this work, provide a linear, anisotropic template for materials processing.

The structure of these dynamic systems is defined by a precarious balance of hydrophobic and electrostatic forces. This balance results in micelle dimensions that are a strong function of system conditions. For example, the length of the micelles increases with increasing surfactant concentration and decreases with increasing temperature.^{8,9} The flexibility and length of wormlike micelles are a function of ionic strength¹⁰ and added polymer, even relatively simple nonionic polymer.^{11,12} Thus, small variations in solution properties affect micelle dynamics and dimensions, limiting many applications of these materials, especially those that involve multistep processing.

To maintain the amphiphilic nature of a wormlike system and generate aggregates with a stable, controllable nanoscale structure, a common approach has been the inclusion of polymerizable moieties and subsequent polymerization to capture the structure.¹³ Polymerizable surfactants have been used in a variety of applications including capturing the structure of spherical micelles^{14,15} and as a stabilizer in emulsion polymerization,^{16,17}

mini-emulsion polymerization,¹⁸ and microemulsion polymerization. Here, we generate amphiphilic polymer–surfactant aggregates through the polymerization of the counterions bound to the surface of cationic surfactant micelles.^{19,20} The resulting polymerized aggregates have a high aspect ratio and are stable over a range of temperatures and concentrations. To utilize these materials, however, greater understanding of their synthesis and independent control of both the radial and length dimension are required. In this work, systematic variation of processing parameters allows for quantification of the effects of varying the micelle template size and polymerization conditions on aggregate dimensions.

Background

Wormlike micelles have been polymerized in systems with both polymerizable surfactants²¹ and polymerizable counterions.^{19,20,22} Here we focus on the ability to control both aggregate dimensions for the latter case. When polymerizing the counterions in a cationic surfactant system, the resulting aggregate consists of a negatively charged “counterion” polymer held in solution by its association with the cationic surfactant. This counterion polymer is formed in the micelle through free radical polymerization of vinyl-containing counterions, and the resulting polyelectrolyte–surfactant aggregates maintain the basic rodlike shape of the pre-reaction micelles, held together by a sterically hindered polymer chain. NMR studies have shown that the polymer is trapped and immobile within the aggregate, whereas the surfactant is still free to dissociate into the bulk aqueous solution.²⁰ Overall, the aggregates remain stable due to the strong hydrophobic and electrostatic attractions between the surfactant

* To whom correspondence should be addressed. E-mail: lwalker@andrew.cmu.edu.

(1) Israelachvili, J. N. *Intermolecular and Surface Forces*; Academic Press: London, 1985.

(2) Gamboa, C.; Rios, H.; Sepulveda, L. *J. Phys. Chem.* **1989**, *9*, 5540.

(3) Gamboa, C.; Sepulveda, L. *J. Colloid Interface Sci.* **1986**, *113*, 566.

(4) Magid, L. J. *J. Phys. Chem. B* **1998**, *102*, 4064.

(5) Rehage, H.; Hoffmann, H. *Mol. Phys.* **1991**, *74*, 933–973.

(6) Cates, M. E.; Candau, S. J. *J. Phys.: Condens. Matter* **1990**, *2*, 6859.

(7) Soltero, J. F. A.; Puig, J. E. *Langmuir* **1995**, *11*, 3337.

(8) Tanford, C. *The Hydrophobic Effect*; Wiley: New York, 1980.

(9) Lequeux, F. *J. Colloid Interface Sci.* **1996**, *1*, 341–344.

(10) Magid, L.; Han, Z.; Li, Z. *Langmuir* **2000**, *16*, 149.

(11) Truong, M. T.; Walker, L. M. *Langmuir* **2002**, *18*, 2024–2031.

(12) Truong, M. T.; Walker, L. M. *Langmuir* **2000**, *16*, 7991–7998.

(13) Paleos, C. M. *Polymerization in Organized Media*; Gordon and Breach: Philadelphia, 1992.

(14) Summers, M.; Eastoe, J.; Davis, S.; Du, Z. *Langmuir* **2001**, *17*, 5388–5397.

(15) Dufour, M.; Guyot, A. *Colloid Polym. Sci.* **2003**, *281*, 97–104.

(16) Green, B. W.; Sheetz, D. P. *J. Colloid Interface Sci.* **1970**, *32*, 96.

(17) Liu, J.; Chem, C. H.; Gan, L. M.; Teo, W. K.; Gan, L. H. *Langmuir* **1997**, *13*, 4988–4994.

(18) Boisson, F.; Uzulina, I.; Guyot, A. *Macromol. Rapid Commun.* **2001**, *22*, 1135–1142.

(19) Kline, S. R. *Langmuir* **1999**, *15*, 2726–2732.

(20) Gerber, M. J.; Kline, S. R.; Walker, L. M. *Langmuir* **2004**, *20*, 8510.

(21) Liu, S. Y.; Gonzalez, Y. I.; Danino, D.; Kaler, E. W. *Macromolecules* **2005**, *38*, 2482–2491.

(22) Kline, S. R. *J. Appl. Crystallogr.* **2000**, *33*, 618–622.

and polymer. Unlike wormlike micelles, the dimensions and structure of the polymerized aggregates are insensitive to changes in temperature and surfactant concentration (above a critical aggregate concentration) because the length is determined by the molecular weight of the stabilizing polymer chain rather than an energetic balance at the end-caps of the micelles.

By polymerizing the counterions, rather than the surfactant, we are able to use a single surfactant template and vary the counterion monomer, allowing for the synthesis of different polymers using this method. The system used in this study is comprised of a series of common cationic surfactants, (C_XH_{2X+1}) -trimethylammonium (where X has values of 14, 16, or 18), with a polymerizable counterion, 4-vinylbenzoate. When mixed in a 1:1 molar ratio, the resulting surfactant, (C_XH_{2X+1}) trimethylammonium 4-vinylbenzoate (C_XTVB), forms a clear, viscoelastic solution of wormlike micelles. After polymerization, the resulting polyelectrolyte-surfactant aggregates are rigid with a cylindrical cross section and a high aspect ratio. The polymerization of the counterion is the most efficient means to produce these polymer-surfactant aggregates. Another approach is to solubilize pre-made poly(4-vinyl benzoate) in a surfactant solution, resulting in stable aggregates which have been observed with light scattering. However, this synthesis route is less desirable because the bulk polymerization of poly(4-vinylbenzoic) acid is slower than polymerization in a micellar template and a second redispersion step would be needed. The in situ polymerization applied here is a single step, efficient process.

Previous work shows that successful $C_{16}TVB$ reactions pass through a turbid phase during polymerization. Small-angle neutron scattering (SANS) experiments suggest that this turbid regime is composed of polymerized rodlike aggregates associating in "bundles" which later dissolve.²² The current work will show that this state does not occur during all reactions and that its existence has no effect on the final product.

Our previous work also shows that the length of the polymerized $C_{16}TVB$ (or $pC_{16}TVB$) aggregates is controlled by varying the concentration of initiator used.²⁰ More specifically, for reaction conditions of 60 °C and $[C_{16}TVB] = 10$ mg/mL, the average polymerized aggregate length, L , is related to the initiator concentration, $[I]$, such that $L \propto [I]^{-0.36}$. In all previous studies of this system, care was taken to fix all other polymerization conditions so that the micelle template length did not change. Due to the sensitivity of the $C_{16}TVB$ structure, the only variable that was investigated without altering the micelle template was initiator concentration. The time scale for breaking and reforming of the micelles ($\sim 10^3$ s⁻¹)¹³ is much faster than the bulk propagation rate for vinyl benzoate (on order 1 s⁻¹ at these concentrations)²³ or even bulk styrene (approximately 4 s⁻¹).²⁴ The template length was therefore assumed to contribute significantly to the resulting degree of polymerization that can be reached and, hence, the length of the resulting aggregates. However, a recent study on a similar system with a polymerizable surfactant showed that the final polymerized aggregate length is longer than the initial micelles, demonstrating the complexity of the competition between reaction kinetics and micelle dynamics.²¹ The current work seeks to elucidate the exact contribution that the template length has to the length of the final product. The outcome of this work is a quantification of the relationship between aggregate length and system variables, including initiator decomposition rate, surfactant concentration, and reaction temperature.

Materials and Methods

Cetyltrimethylammonium hydroxide and 4-vinylbenzoic acid were purchased from Fluka (Ronkonkoma, NY). D₂O, 99.9 mol % enriched, potassium bromide, and potassium bromate were purchased from Sigma-Aldrich (St. Louis, MO). Myristyltrimethylammonium bromide ($C_{14}TAB$), methanol, and Dowex 550 microsphere ion exchange resin were purchased from Fisher Scientific (Houston, TX). Octadecyltrimethylammonium chloride ($C_{18}TAC$) (Arquad 18-50) was donated by Akzo-Nobel (Chicago, IL). The water-soluble free-radical initiator VA-44 (2,2'-azobis[2-(2-imidazolin-2-yl)propane] dihydrochloride) was donated by Wako Chemicals (Richmond, VA). The second initiator used, Vazo-56 (2,2'-azobis(2-amidino-propane) dihydrochloride) was purchased from DuPont (Wilmington, DE). The two initiators will be referred to as V-44 and V-56, respectively. All materials were used as received. Water from a reverse osmosis source was purified in a Millipore filtration system immediately before use.

$C_{14}TAB$ was converted to the hydroxide form, $C_{14}TOH$, by passing a 10 wt % solution of $C_{14}TAB$ in methanol through a column of Dowex ion-exchange resin three times. The ion exchange was confirmed at the exit of the column by observing a shift to a pH greater than 12.5. Conversion to the hydroxide counterion was further confirmed through a Volhard titration for bromide.²⁵ The $C_{14}TOH$ was dried in a vacuum oven and then freeze-dried to recover the surfactant as a powder. $C_{18}TAC$ was dried from the received Arquad solution in a vacuum oven and converted to $C_{18}TOH$ in the same manner.

(C_XH_{2X+1}) trimethylammonium 4-vinylbenzoate (C_XTVB), the polymerizable form of the three surfactants, was prepared by neutralization of 4-vinylbenzoic acid in the presence of a slight stoichiometric excess of C_XTAOH using a method described elsewhere.^{19,20} The neutralization is performed in cold water, and the difference in Krafft temperature between C_XTVB and C_XTAOH is used to separate the surfactant crystals. Ethylene glycol must be added to the $C_{14}TVB$ solution in order for the Krafft temperature ($T_k \sim -5$ °C) to be approached without freezing. Once the C_XTVB is precipitated, it is washed three times with deionized water and then freeze-dried. The molecular composition of surfactants prepared using this procedure has been confirmed using NMR and shown to be free of impurities.²⁰

Samples for polymerization were prepared with water which was boiled for 10 min to remove residual CO₂ and then cooled under nitrogen (grade 5.0) to deplete any oxygen. The surfactant was dissolved and allowed to equilibrate at the reaction temperature with light stirring under an atmosphere of continuously circulating nitrogen which had been bubbled through water. Three reaction temperatures were used: 48, 60, and 70 °C. These temperatures were chosen such that the decomposition rates of the two initiators overlap. The reaction was initiated by injecting 1 mL of initiator predissolved in water into the homogeneous surfactant solution. Initiator concentration, $[I]$, will be defined as the mole percent initiator relative to moles of surfactant. Most polymerizations were carried out using a constant initiator concentration of $[I] = 2.5\%$. One sample was polymerized using $[I] = 0.5\%$. Three different $C_{16}TVB$ concentrations were used: 10, 5, and 1.25 mg/mL corresponding to concentrations of 23, 11.5, and 2.9 mM, respectively. Reactions using $C_{14}TVB$ and $C_{18}TVB$ were performed using 5 mg/mL of surfactant, or 12.3 mM and 10.8 mM, respectively. The reactions were run in a pure nitrogen atmosphere and under constant stirring using a magnetic stir bar. Successful reactions using 10 mg/mL C_XTVB were observed to pass through a turbid phase during the course of the reaction. Samples using lower concentrations of C_XTVB showed no observable turbidity during the reaction. The polymerized aggregate product is a clear solution exhibiting none of the viscoelasticity of the initial solution and which does not precipitate when chilled below the Krafft temperature of C_XTVB .

To determine the conversion of vinyl groups in the polymerization reaction, a bromine titration was used. Standard bromine solutions

(23) Kamachi, M.; Satoh, J.; Liaw, D. J.; Nozakura, S. *Macromolecules* **1977**, *10*, 501-502.

(24) Madruga, E. L. *Makromol. Chem. Rapid Comm.* **1993**, *14*, 581-589.

(25) Harris, D. C. *Quantitative Chemical Analysis*; W. H. Freeman and Co.: New York, 1996.

were prepared by mixing potassium bromate with 10 times excess potassium bromide. The bromine was titrated into solutions of pC₁₆TVB until the pale yellow end point was detected using a Spectronic Genesys 2 UV–vis spectrophotometer, measuring the absorbance at a wavelength of 420 nm. Back-titration or iodometric titration is not possible because iodine binds irreversibly with the C₁₆TA⁺ surfactant and forms an insoluble precipitate. The concentrations of standard solutions of unpolymerized C₁₆TVB were measured with an accuracy of $\pm 1\%$, indicating that the presence of vinyl groups within the micelle does not hinder this technique. The minimum detectable concentration of vinyl groups using this method is 45 $\mu\text{g/mL}$ or 0.1 mM.

Previous work has made use of static light scattering (SLS) to determine aggregate length. However, the longer aggregates produced in this study are too large for the Debye approximation inherent to SLS calculations to be valid. Thus, for this work, dynamic light scattering (DLS) is employed. DLS experiments were performed using a Brookhaven Instruments Corporation BI-200SM goniometer with a $\lambda = 532$ nm laser source. Experiments were performed with a temperature of 25 °C and a sample concentration of 0.5 mg/mL. The decay time, Γ , was measured over a range of scattering angles from 60 to 130° at 10° intervals and shown to be a linear function of q^2 . An extrapolation of these data passes through the origin, indicating that the contribution of rotational diffusion to the measured diffusivity is negligible and that the measured diffusivity is dominated by translational diffusion. Thus, for all samples, the reported sizes are derived from DLS at a single angle (90°). In addition, there is no concentration dependence to the scattering in the dilute regime. Samples were allowed to correlate for at least 6 min, using an initial delay of 1.0 μs and a final delay of 100 ms. The resulting correlation function was analyzed using the CONTIN method²⁶ to provide the best fit size distribution with an average hydrodynamic radius, $\langle R_h \rangle$. The effective translational diffusion coefficient, D_T , from the CONTIN analysis was used to calculate the average length of the aggregates using the Broersma relationship for diffusion of rods^{27,28}

$$D_T = \frac{kT}{3\pi\eta_0 L} \left[\ln\left(\frac{2L}{d}\right) - \xi \right] \quad (1)$$

where k is the Boltzmann constant, T is the absolute temperature, η_0 is the viscosity of the solvent (water), L is the aggregate length, d is the aggregate diameter (measured with SANS), and ξ is a correction for the finite length of the rod. Several formulations for ξ are available;^{27–30} we use the function of Newman et al. as it is most relevant in the aspect ratio range explored in this work.²⁹ For DLS, each sample was run at least 10 times, and the resulting lengths were averaged. The resulting size distributions were manually averaged using the following procedure. A spline fit of each distribution was used to evenly space the x values. These fits were normalized such that the integral under each curve was equal to unity, and the 10 resulting curves were then averaged at each value of x producing a single, composite curve. This curve was then normalized such that the highest point represented a distribution value of one hundred.

Rheological experiments were performed on a Rheometric Scientific ARES strain-controlled rheometer using a Couette (cup and bob) geometry. The bob has a length of 33 mm, a radius of 16 mm, and a gap of 1 mm. The temperature of the sample was maintained using a circulating fluid bath. The rheometer was allowed to equilibrate at the experimental temperature for at least 30 min. Temperature equilibration and the relaxation of loading stresses were ensured by measuring the moduli at a fixed frequency and strain amplitude ($\gamma = 10\%$, $\omega = 10$ rad/s) as a function of time to verify time independent values. Once equilibrated, frequency sweeps were performed using 10% strain (shown to be in the linear regime)

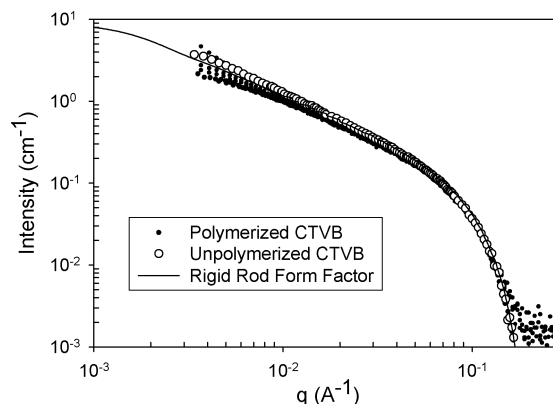


Figure 1. Small angle neutron scattering spectra of C₁₆TVB (open symbols) and pC₁₆TVB (closed circles) polymerized under various conditions. Also shown is the rigid rod form factor for an infinite cylinder with radius 2 nm (solid line). The polymerized samples from top to bottom are as follows: 2.5% V-56; 48 °C; 10 mg/mL C₁₆TVB, 2.5% V-44; 60 °C; 5 mg/mL C₁₆TVB, 2.5% V-44; 48 °C; 10 mg/mL C₁₆TVB, 1.0% V-54 60 °C; 10 mg/mL C₁₆TVB.

and frequencies ranging from 10² to 10^{−3} rad/s. Steady-state behavior was used to characterize lower viscosity samples; a steady shear rate was applied until the sample reached a stable value of stress.

Small angle neutron scattering (SANS) experiments were performed on the NG3 30 m SANS instrument at the NIST Center for Neutron Research in Gaithersburg, MD. A 1.2 cm diameter, collimated beam of neutrons of wavelength $\lambda = 6$ Å ($\Delta\lambda/\lambda = 0.143$) were incident on 2 mm thick samples in quartz cells. SANS data is presented as scattered intensity as a function of normalized scattering angle q , defined as $q \equiv 4\pi/\lambda \sin(\theta/2)$ where λ is the wavelength of incident radiation and θ is the scattering angle. Two sample-to-detector distances were used to give an overall q range of $0.0037 < q < 0.23$ Å^{−1}. Sample scattering was corrected for background and empty cell scattering. The corrected data sets were circularly averaged and placed on an absolute scale using procedures and software supplied by NIST.

Results

Determination of Aggregate Radius. The impact of the polymerization reaction on the radius of the polymerized aggregates was first determined. Figure 1 shows the scattering intensity, $I(q)$, dependence of neutron scattering for unpolymerized C₁₆TVB compared to a number of different polymerized aggregate samples, with a solid line representing the monodisperse rigid rod form factor for an infinite cylinder of radius 2 nm.^{31,32} The aggregates were polymerized using a wide range of reaction conditions, including varied initiator concentration, surfactant concentration, and temperature. All data were taken using a dilute sample concentration of 1 mg/mL. For all cases, the data collapse onto a single curve at $q > 0.02$ Å^{−1}. This range of scattering angle probes the cross-sectional dimension, or the radius, of the C₁₆TVB micelles and polymerized aggregates. Over this range ($q > 0.02$ Å^{−1}), the overlapping curves in Figure 1 are well described by a monodisperse rigid rod form factor for an infinitely long cylinder of radius 2.0 nm. Thus, the initial micelle radius is unperturbed by the polymerization reaction, regardless of the reaction conditions used. Previous work on rodlike micelles with carboxylate containing aromatic counterions has shown that the aromatic group resides at the organic/water interface, with, in this case, the vinyl group extending into the core of the micelle.^{20,33} Thus, since the radial dimension does not change with polym-

(26) Provencher, S. W. *Comput. Phys. Commun.* **1982**, 27, 213–242.

(27) Broersma, S. J. *J. Chem. Phys.* **1960**, 32, 1626–1635.

(28) Broersma, S. J. *J. Chem. Phys.* **1981**, 74, 6989–6990.

(29) Newman, J.; Swinny, H. L.; Loren, D. A. *J. Mol. Biol.* **1977**, 116, 593–606.

(30) Tirado, M. M.; Torre, J. G. d. I. *J. Chem. Phys.* **1979**, 71, 2581–2589.

(31) Fournet, G. *Bull. Soc. Fr. Mineral. Crist.* **1951**, 74, 37–172.

(32) Higgins, J. S.; Benoit, H. C. *Polymers and Neutron Scattering*; Clarendon Press: Oxford, U.K., 1994.

(33) Rikitin, A. R.; Pack, G. R. *Langmuir* **2005**, 21, 837–840.

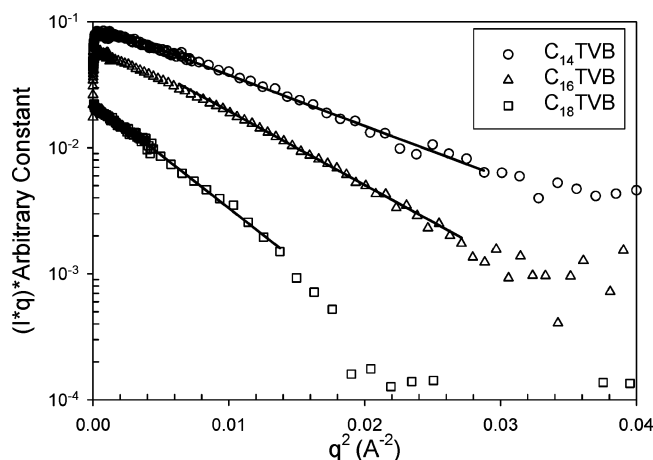


Figure 2. Gunier plot of SANS data from three surfactants. From the linear fits we extract radii of 1.7 ± 0.1 , 2.0 ± 0.1 , and 2.4 ± 0.1 nm, for C_{14} TVB, C_{16} TVB, and C_{18} TVB, respectively. The data have been vertically shifted to aid viewing, and the lines indicate the range of the linear fit.

erization, we may assume that the polymer retains its position inside the micelle core.

Since the aggregate radius is determined solely by the radius of the template micelle, we can vary this accurately by changing the surfactant tail length used. To vary the radius of the polymerized micelles, two new surfactants, C_{14} TVB and C_{18} TVB, were prepared. As with C_{16} TVB, both of these surfactants form highly viscoelastic solutions of wormlike micelles with the viscosity of the solution increasing qualitatively with increasing tail length. This observation is expected because surfactants with longer hydrophobic tails have a lower CMC resulting in longer micelle lengths at a given surfactant concentration.³⁴ The three surfactants were polymerized using 5 mg/mL of surfactant and 2.5% VA-44 at 60 °C to quantify the effect of micelle tail length on the final aggregate radius.

Figure 2 shows a Gunier representation of the SANS results from the three surfactants. For a rodlike particle, the slope of the high- q linear portion of this graph is directly related to the radial dimension of the aggregate.³² The radii measured for C_{14} TVB, C_{16} TVB, and C_{18} TVB are 1.7 ± 0.1 , 2.0 ± 0.1 , and 2.4 ± 0.1 nm, respectively. As expected, the radius increases monotonically with increasing surfactant tail length. For every two carbons added to the surfactant tail, the radius of the aggregates increases by 3–4 Å. Thus, we have a method for controlling the radius of these aggregates.

The measured radii and rodlike nature of these particles is confirmed by analysis of the neutron scattering for the three surfactant aggregates. Figure 3 shows the scattering intensity, $I(q)$, as a function of the scattering vector, q , for the three samples. The solid lines are rigid rod form factor models of the scattering based on the radius measured using the Gunier plot. The model fits the scattering well for most of the q range, confirming the reported radii. The negative one slope in the intermediate q range indicates the presence of long regions of rigidity in the aggregates, confirming for all surfactants that the rodlike shape is maintained. The low- q data shows deviations from the rigid rod model. At the surfactant concentration for which this SANS was performed, however, the effects of polydispersity, flexibility, and charge interactions on the low- q scattering cannot be separated or uniquely identified. Thus, this region of the scattering curve in Figure 3 is not analyzed through scattering models, and the

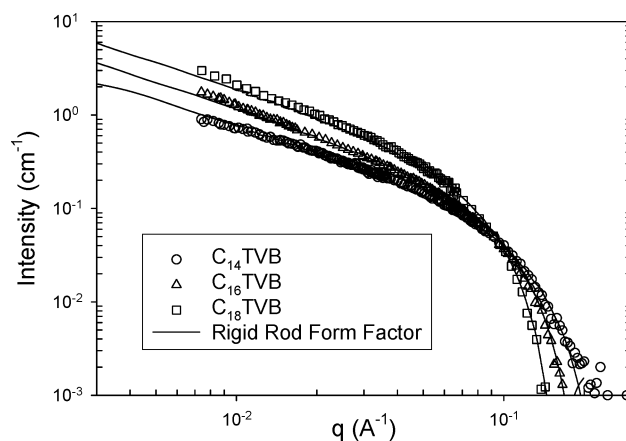


Figure 3. SANS for micelles with varying surfactant tail lengths. The solid lines represent rigid rod form factor scattering predictions based on the values for radius given in Figure 2.

aggregate length is determined from light scattering. Nonetheless, when compared with Figure 1, this plot shows clearly that the radial cross-section of the aggregates can be varied.

Varying the Template Length. Wormlike micelles are very sensitive to solution conditions, and thus the length of the unpolymerized micellar template is easily varied. In this work, changes in both temperature and surfactant concentration are used to change the template length. The simplest way to qualify these effects is through the rheology of C_{16} TVB solutions. Like many wormlike, entangled micelles, C_{16} TVB is viscoelastic and strongly shear thinning.^{5,6} Assuming a flexible micelle in the fast-breaking regime, the zero shear viscosity is roughly proportional to the micelle length.³⁵ In other regimes of micelle dynamics, the dependence of viscosity on micelle length only becomes stronger, whereas for more rigid systems, the viscosity is proportional to rod length squared.³⁶ In this work, viscosities were determined using two methods. For higher viscosity samples, a frequency sweep was performed using oscillatory shear at fixed strain amplitudes within the linear limit. The frequency dependence of the elastic modulus, G' , and the viscous modulus, G'' , show the single-relaxation-time dominated behavior often observed for wormlike micelle systems.³⁵ The complex viscosity reaches a plateau value at low shear rates, allowing for an extrapolation to the zero deformation viscosities reported here. For the less viscous solutions, experiments were performed using steady shear. The applied shear rate was varied until the zero shear viscosity was identified. Between 40 and 50 °C, both methods are used to characterize the viscosity and are found to provide similar values. The viscosity reported is either the zero-shear rate or zero-frequency value.

Figure 4 shows the viscosity of C_{16} TVB as a function of temperature for samples with two different surfactant concentrations, 5 and 10 mg/mL. The figure shows the strong effect of varying temperature and concentration on the micelle rheology and, therefore, the template length. The solid line represents a fit of the data assuming that the viscosity is determined by the sum of the contributions from the micelles and the solvent (water), such that

$$\eta(T) = Ae^{E_M/RT} + \eta_w(T) \quad (2)$$

where E_M is the activation energy of the viscosity of the micelle solution, R and T are the gas constant and absolute system

(34) Hamley, I. W. *Soft Matter: Polymers, Colloids, Amphiphiles, and Liquid Crystals*; John Wiley & Sons: Chichester, U.K., 2000.

(35) Kern, F.; Lequeux, F.; Zana, R.; Candau, S. J. *Langmuir* **1994**, *10*, 1714–1723.

(36) Dhont, J. K. G.; Briels, W. J. *Colloids Surf., A* **2003**, *213*, 131–156.

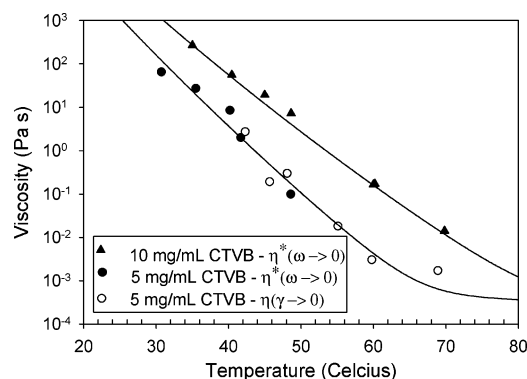


Figure 4. Viscosity of C_{16} TVB solutions as a function of temperature at two surfactant concentrations. The lines indicate the best fit of eq 2.

temperature respectively, A is a scaling constant, and η_w is the viscosity of water as a function of temperature.³⁷ By fitting the high viscosity samples, where the micelle rheology dominates, E_M is found to be 254.3 kJ/mol for 10 mg/mL C_{16} TVB and 297.9 kJ/mol for 5 mg/mL C_{16} TVB. These activation energies are consistent with those reported for other micellar systems, which range from 70 to 300 kJ/mol.^{6,35,38–41} This represents a strong dependence on temperature such that a 10° decrease in temperature causes a 10-fold increase in the viscosity. In this work, the temperature of the micelle reaction was varied from 48 to 70 °C, representing, a 1000-fold change in viscosity and, therefore, an enormous change in the template length. In addition, for wormlike micelles, a change in surfactant concentration affects the length of micelles formed.⁶ For the case of C_{16} TVB, a decrease from 10 to 5 mg/mL results in a 100-fold decrease in viscosity. The strong dependence of the length of the micelle template on surfactant concentration and temperature will be utilized to vary this length and determine its effect on the dimensions of polymerized C_{16} TVB aggregates.

Our previous work varied only the concentration of initiator used, the one reaction condition that has no effect on the micelle template.²⁰ To change the micelle template independently of reaction conditions, the surfactant concentration during the reaction was varied. Three C_{16} TVB concentrations were used: 10.0, 5.0, and 1.25 mg/mL. In addition, to provide multiple points of comparison, reactions were carried out at three temperatures for each surfactant concentration: 48, 60, and 70 °C. In all cases, the initiator, V-44, was kept at a constant molar ratio with respect to C_{16} TVB of $[I] = 2.5\%$. Thus at a specific temperature, the three C_{16} TVB concentrations are assumed to experience the same reaction rate. Transport of the initiator could be influenced by the change in solution viscosity, but we do not expect that this would have a significant effect on the overall reaction kinetics.

Figure 5 shows the average lengths of polymerized aggregates formed when varying temperature at three different starting surfactant concentrations as measured using dynamic light scattering (DLS). The solid lines are present simply to guide the eye. After polymerization, all samples were diluted to 0.5 mg/mL, the concentration at which DLS experiments were performed. Previous work has shown that the aggregate dimensions are insensitive to dilution at this concentration.¹⁹ The dimensions provided are the weight-average lengths obtained from multiple

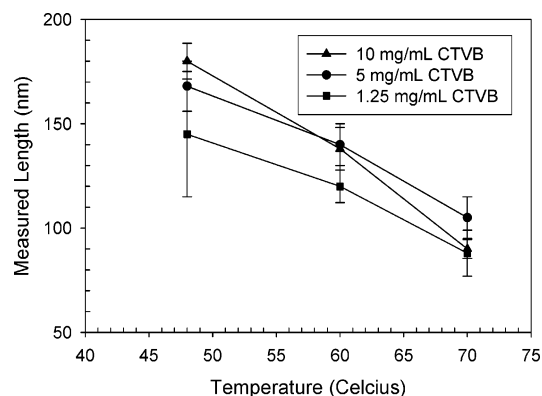


Figure 5. Length of polymerized aggregates (DLS) as a function of polymerization temperature for three different initial surfactant concentrations. All DLS experiments were performed using a polymerized aggregate concentration of 0.5 mg/mL.

runs of a CONTIN analysis, and the error shown is the standard deviation of the mean of at least 10 repetitions for each point. One should note that polyelectrolyte scattering often results in “slow modes” which can skew a molecular weight distribution to higher size values.^{42,43} The correlation functions for our samples, however, do not show evidence of these slow time scales, most likely because polymer charge concentration is equivalent to the added “salt” (in this case surfactant).

The effect of varying the initial micelle length is determined by examining the data at a given temperature, i.e., the dependence of final length on surfactant concentration, representing three different starting template lengths. The temperature dependence of the aggregate length is more complicated, as it involves variations in both the starting micelle length and the reaction rate, and it will be discussed later. In Figure 5, the aggregate lengths resulting from polymerizations at a given temperature using surfactant concentrations of 10 and 5 mg/mL are statistically identical, with the errors in the measurement overlapping over a wide range. For example, for aggregates polymerized at 60 °C, the 10 mg/mL C_{16} TVB sample has an average length of 138 ± 10.2 nm, whereas the 5 mg/mL C_{16} TVB sample has an average length of 140 ± 10.0 nm, statistically the same value. Thus, even with the large shift in template length, evidenced by the system rheology shown in Figure 4, there is no apparent effect on the polymerized aggregate. For this concentration range, the final product is independent of the surfactant concentration used. As in previous studies, the 10 mg/mL sample is observed to pass through a turbid phase during the reaction. The samples at lower concentrations, however, remained clear for the entire reaction. Thus, the observation of a turbid phase during the reaction has no effect on the final product, as both the 10 and 5 mg/mL polymerization are identical.

The samples polymerized from a 1.25 mg/mL C_{16} TVB solution appear to have a shorter average length at all three temperatures studied. At 1.25 mg/mL (18 times the cmc), the wormlike micelle solutions are viscoelastic even at higher temperatures, indicating that the template is still long enough to be entangled. This shorter length of the resulting aggregates is due to a lack of complete conversion of these samples. Table 1 shows the conversion of vinyl groups for all pC_{16} TVB samples measured using a bromine titration. Polymerization of $[C_{16}TVB] = 10$ or 5 mg/mL achieve essentially complete conversion, with measured conversions near 99%. Polymerizations using 1.25 mg/mL C_{16} TVB, however, had

(37) Bingham, E. C. *Fluidity and Plasticity*; McGraw-Hill Book Co.: New York, 1922.

(38) Raghavan, S. R.; Kaler, E. W. *Langmuir* **2001**, *17*, 300–306.

(39) Prasad, C. D.; Singh, H. N. *Colloids Surf.* **1990**, *50*, 37–45.

(40) Candau, S. J.; Hirsch, E.; Zana, R.; Delsanti, M. *Langmuir* **1989**, *5*, 1225.

(41) Berret, J. F.; Porte, G.; Decruppe, J. P. *Phys. Rev. E: Stat., Nonlinear, Soft Matter Phys.* **1997**, *55*, 1668.

(42) Foerster, S.; Schmidt, M.; Antonietti, M. *J. Phys. Chem.* **1992**, *96*, 4008.

(43) Beer, M.; Schmidt, M.; Muthukumar, M. *Macromolecules* **1997**, *30*, 8375–8385.

Table 1. Final Conversion of Vinyl Groups in the Aggregate Product as Measured Using a Bromine Titration^a

temperature (°C)	[C ₁₆ TVB] (mg/mL)		
	10	5	1.25
48	99.3	98.2	91.9
60	98.7	97.8	94.6
70	98.9	98.6	95.5

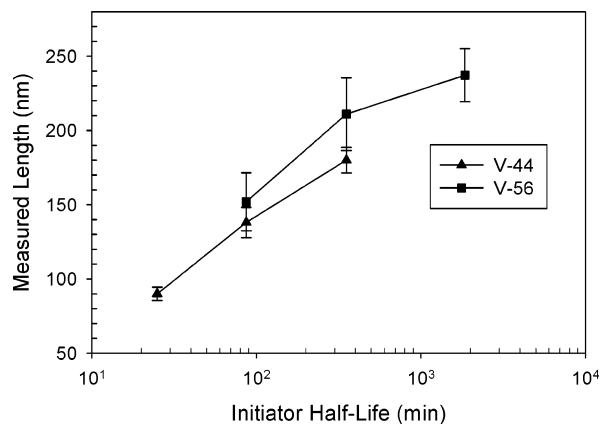
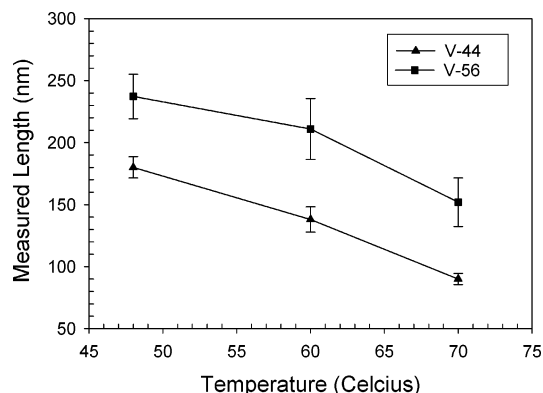
^a Temperatures and concentrations refer to the conditions during the polymerization.

only 92–96% conversion. Thus, there is a population of unpolymerized 4-vinyl benzoate counterions in solution with the polymerized aggregates. We expect this free counterion leads to the formation of small micelles thereby lowering the average length measured with DLS. The 1.25 mg/mL sample polymerized at 70 °C had the highest conversion and also the length closest to those of the aggregates formed using higher surfactant concentrations. Clearly, the reaction must reach essentially full conversion in order for the maximum average aggregate lengths to be achieved for a given set of conditions.

Controlling Aggregate Length with Initiator Half-Life. Our previous work showed that varying the concentration of initiator during the polymerization reaction is an effective method of controlling the lengths of the aggregates produced.²⁰ This technique is limited by the diffusion of the initiator at low concentrations. It is successful for concentrations of V-44 of [I] = 0.5% (mole percent relative to the monomer) or higher, resulting in polymerized aggregates with a maximum length of 240 nm. To synthesize aggregates of greater length, we would want to minimize the initiator half-life without hindering the reaction by lowering the initiator concentration.

The half-life of the initiator can be varied in two ways. First, the initiator itself can be changed. In this study, two initiators are used: V-44 and V-56. Both have similar chemistries and produce free radicals by the same mechanism. The rate of this decomposition is a function of temperature and is faster for V-44 than for V-56. The only other difference between the molecules is that, based on functional groups present, V-44 is slightly more soluble in the micelle core, though both are highly soluble in water. The second method for varying the initiator half-life is to change the reaction temperature. As temperature decreases, so does the rate of decomposition, which results in longer polymerized aggregates, as evidenced in Figure 5. Since temperature also affects the template length, however, its exact effect on product dimensions is more complicated to predict than other variables studied thus far.

Figure 6 shows the lengths of aggregates polymerized using two different initiators as a function of initiator decomposition half-life. The lengths increase monotonically with increasing half-life, as one might expect for a typical free radical polymerization.⁴⁴ Longer half-lives result in a smaller supply of free radicals, having the same effect as decreasing the overall initiator concentration and resulting in longer polymers and aggregates. At a given half-life, the aggregates polymerized using V-56 are longer than those polymerized using V-44. This observed increase in size is most likely due to the difference in solubilities of the two initiators in the micelle core rather than changes in the micelle template. At a given half-life, the V-56 aggregates are polymerized at a higher temperature, since the initiator decomposition is slower. Thus, the V-56 aggregates are polymerized from a micelle which is initially shorter than a V-44 aggregate at the same half-life. The observed slight increase in

**Figure 6.** Aggregate lengths (DLS) as a function of initiator half-life for two different initiators.**Figure 7.** Aggregate length (DLS) as a function of reaction temperature for two different initiators.

size when using V-56 is contrary to the trend in template length and we attribute it to initiator solubility in the micelle core.

Figure 7 shows the same data as Figure 6 but plotted as a function of reaction temperature. From the DLS results, it is clear that the aggregate length is controlled by the reaction temperature, but the variation in aggregate lengths is much smaller than changes in the length of the micelle template over the same temperature range (see Figure 4). Over this range, the lengths of the polymerized aggregates are changed by about a factor of 2, whereas by the most conservative estimate, the initial micelle lengths can be changed by at least an order of magnitude. Thus, the increase in aggregate length with decreasing temperature is dominated by the slowing of initiator decomposition, with only an incidental, if any, contribution from the increased template length.

Discussion

We have shown that the length of pC₁₆TVB aggregates is controlled by the reaction conditions, with the initial micelle template length having essentially no effect. The propagation step of the reaction is assumed to be very fast, since there is a high local concentration of monomer in the micelle core. In addition, these monomers are organized along the micelle backbone, allowing for an efficient propagation. This effect is very pronounced, with other polymerizable surfactant systems having observed propagation rates on the order of 10⁵ s⁻¹.¹³ Even with varying temperature, this rate is much faster than the fastest initiator decomposition rate used in this study (~10⁻³ s⁻¹).⁴⁵ Thus, the kinetics of the initiation step is the rate-limiting step of the C₁₆TVB polymerization.

(44) Flory, P. J. *Principles of Polymer Chemistry*; Cornell University Press: Ithaca, NY, 1953.

(45) DuPont. *Vazo free radical product info*.

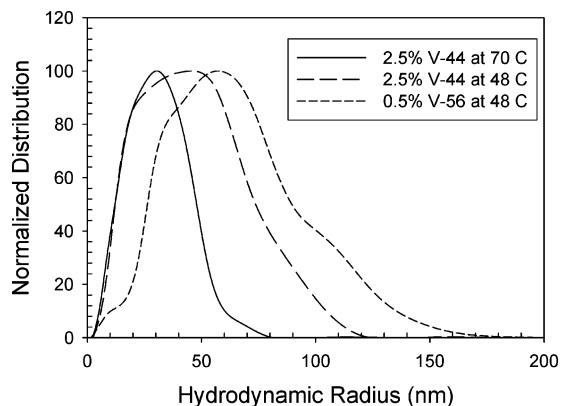


Figure 8. Distribution of particle size (DLS) for samples polymerized using three different reaction conditions.

In this study, the reaction kinetics is controlled by varying the initiation step: either by varying the initiator concentration or the initiator decomposition half-life. The limits of varying initiator concentration were probed in previous work.²⁰ The practical low limit of initiator concentration is $[I] = 0.25\%$, the point at which diffusion starts to hinder the reaction, and the high limit is $[I] = 10\%$, the point at which reaction conversion begins to suffer due to the generation of a predominance of short oligomers. Within this range, aggregates can be produced with lengths between 90 and 340 nm (measured by a combination of SLS and SANS). Variation of initiator half-life offers an alternate route for controlling the micelle length, as shown in Figure 6. By simply varying the reaction temperature, a similar range of lengths of aggregates are produced. Smaller aggregates are obtained by reacting $C_{16}TVB$ at higher temperatures, as long as the temperature is lower than the boiling point of the solvent. Conversely, reactions performed using a low initiator concentration and a low-temperature result in even longer aggregates. For example, a polymerization using 0.5% V-56 at a reaction temperature of 48 °C yields aggregates with lengths of approximately 500 nm. However, lowering the temperature can present processing challenges. Figure 4 shows the strong temperature dependence of the system viscosity. At low temperatures, the high viscosity of the solution hinders both mixing and diffusion of initiator. This challenge can be overcome by lowering the surfactant concentration in the reactor, thereby lowering the solution viscosity.

Over a wide range, variation of the surfactant concentration has no effect on the final product of the reaction, as evidenced by the $[C_{16}TVB] = 10$ and 5 mg/mL data on Figure 5. Generally, the reaction can be performed at any convenient surfactant concentration such that solution viscosity and yields are optimized for a given desired aggregate dimension. Although the low limit of surfactant concentration would ideally be the cmc, the practical limit in this case is approximately 1.25 mg/mL, the concentration below which reaction conversion is hindered. The longest aggregates are therefore produced by performing reactions using low initiator concentration, temperatures, and surfactant concentrations.

The cost of this approach is that slowing the reaction rate increases the polydispersity of the product. Much like an emulsion polymerization, for which a longer nucleation time results in greater polydispersity,¹³ slower initiator decomposition rates result in a broader particle size distribution. Figure 8 shows the composite particle size distribution from a DLS analysis for three different polymerized $C_{16}TVB$ aggregate samples. Each distribution represents the average of 10 separate DLS correlations. For the two samples polymerized using the initiator V-44,

a decrease in reaction temperature results in a significant broadening of the distribution in addition to the increased average size. For aggregates polymerized at 48 °C, most of the smaller rod lengths produced when running the reaction at 70 °C are still represented. Thus, although lowering the temperature (or increasing the initiator decomposition half-life) does result in a longer average aggregate size, the polydispersity of the product is increased. This effect is even more apparent for samples polymerized using V-56. As Figure 8 shows, the reaction which produced the aggregates with the longest average size (0.5% V-56 at 48 °C) also resulted in the broadest distribution. The increased polydispersity observed for reactions with slower initiator decomposition rates also explains the large error bars for the V-56 samples in Figure 6, as broader distributions adversely affect the reproducibility of a CONTIN analysis. The observed polydispersity represents another processing challenge. For example, to produce a monodisperse particle with very long length, some fractionation would be required. However, since the polymerization, and not the template or micelle dynamics, dictates the final length of the aggregates, other polymerization chemistries that provide more control over molecular weight distribution are feasible in this system.

Aside from greater flexibility in processing decisions, the independence of the reaction with respect to surfactant concentration also allows us to explain the nature of the turbidity observed when $C_{16}TVB$ is polymerized at concentrations greater than 5 mg/mL. We hypothesize that the observed turbid regime is the result of a temporary phase separation between polymerized aggregates and unpolymerized micelles. Turbidity during a reaction is observed to occur at times roughly equivalent to monomer conversions between 50 and 90%.²² Since the initiation step is the rate-limiting step of the reaction and propagation is very fast, at 50% conversion, the solution should have two populations: completely polymerized aggregates (only 1–2 chains are necessary for aggregate stability) and free micelles (the intermediate state being very rare). As previously noted, these two populations would exist with two vastly different length scales. In addition, unpolymerized $C_{16}TVB$ exhibits stronger charge interactions than the polymerized aggregates, as evidenced by the presence of a Coulomb interaction peak in more concentrated SANS experiments.¹⁹ Thus, during the polymerization, a bimodal distribution exists consisting of long, flexible, and charged micelles as well as shorter, more rigid, and more neutral aggregates. The resulting phase separation is therefore not surprising. However, a critical concentration of aggregates is required to drive phase separation, evidenced by its absence in low-surfactant concentration reactions. Since the separated material has already reached full conversion, it does not affect the progress of the reaction, supported by the observation that the final lengths obtained are constant irrespective of the observation of turbidity during the reaction. The separated material redissolves readily as more monomer is converted (and the proportion of charged, wormlike micelles decreases) and a homogeneous solution of polymerized aggregates is achieved. The turbidity appears to be a temporary phase separation of two types of aggregates in solution; the hypothesis above is just one possibility, and others are just as likely. One proposed mechanism for the formation of the turbid phase is that the polymerized micelles aggregate into large bundles.²² Another possibility is the formation of a nematic phase, but we have not observed any birefringence in the sample to indicate the presence of an ordered phase of the polymerized aggregates.⁴⁶ Regardless of the nature

(46) Kumar, S. *Liquid Crystals: experimental studies of physical properties and phase transitions*; Cambridge University Press: New York, 2001.

of the phase separation, however, it is temporary and does not impact the final aggregate structure.

Conclusions

We have elucidated the parameters necessary to independently control the final radius and length of rodlike polymerized aggregates. The radial dimension is not affected by reaction conditions and is determined solely by the initial radius of the micelle template. This can be varied by choosing surfactants with different tail lengths. Conversely, the length of the aggregate is independent of the template and is determined by the reaction conditions used. This fact allows surfactant concentration to be a free variable, as it has no effect on the outcome of the reaction. The highest usable concentration is limited practically by the high viscosities of wormlike micelles, which would hinder diffusion and mixing, and the theoretical low concentration limit is the cmc (practically, however, achieving complete conversion here would represent a processing challenge). Therefore, the reaction can be carried out over a wide range of surfactant concentrations chosen based on convenience.

The aggregate length is controlled by varying the initiator concentration or the half-life of initiator decomposition (by varying temperature and the initiator chosen). This method has been used to polymerize pC₁₆TVB with lengths between 80 and 500 nm. Longer polymerized aggregates are obtained by operating

the reaction at low initiator concentrations and initiator decomposition rates. The cost of this approach is a broadening of the size distribution. Even so, lowering the polymerization temperature is the best method for generating the longest aggregates. Since this process is insensitive to template length, the surfactant concentration can be lowered to avoid any mixing problems arising from increased viscosity at lower temperatures. Ideally, stable amphiphilic rods of micron length should be obtainable. The resulting long, linear hydrophobic regions offer a unique environment for templating or as a sight for organic phase polymerizations.

Acknowledgment. Special thanks to Dr. Steven R. Kline for many meaningful conversations. This work was supported by the National Science Foundation CTS-0092967. Light scattering equipment was provided by a grant from the PPG foundation. This work utilized facilities supported in part by the National Science Foundation under Agreement No. DMR-9986442. Certain trade names and company products are identified in order to specify experimental procedures adequately. In no case does such identification imply recommendation or endorsement by the National Institute of Standards and Technology, nor does it imply that the products are necessarily the best available for the purpose.

LA052297Q